

# Gaussian-induced rotation in periodic photonic lattices

Dragana M. Jović,\* Slobodan Prvanović, Raka D. Jovanović, and Milan S. Petrović

*Institute of Physics, P.O. Box 57, 11001 Belgrade, Serbia*

\*Corresponding author: jovic@phy.bg.ac.yu

Received February 2, 2007; revised March 28, 2007; accepted April 26, 2007;  
posted May 4, 2007 (Doc. ID 79652); published June 21, 2007

We numerically investigate time-dependent rotation of counterpropagating mutually incoherent self-trapped Gaussian beams in periodic optically induced fixed photonic lattices. We demonstrate the relation between such rotation and less confined discrete solitonic solutions. © 2007 Optical Society of America  
OCIS codes: 190.5330, 190.5530.

Light propagation in periodic photonic structures has attracted growing interest to both fundamental physics and applications in recent years [1–5]. Optically induced photonic lattices (PLs) provide an excellent opportunity for studying many interesting phenomena of light propagation balanced between discreteness and nonlinearity. Some of them are the intrinsic localized modes, so-called discrete or lattice solitons [6–10]. Another interesting phenomenon attractive for all-optical manipulation of light is soliton rotation, theoretically considered [11] and experimentally confirmed [12] in the Bessel-like ring lattices. In addition, soliton rotation can be found in other diverse fields, such as Bose–Einstein condensates, but also in *radially* periodic potentials (lattices) [13]. We numerically investigated vortex-induced rotating structures [14], but in *periodic* PLs. Here, we demonstrate, for the first time to our knowledge, Gaussian-induced rotation in these PLs and discuss its relation with less confined discrete solitons.

In this Letter, we report a numerically time-dependent stable rotating beam structure, resulting from the collision of two counterpropagating (CP) mutually incoherent self-trapped Gaussian beams in periodic optically induced fixed PLs. Bifurcation from Gaussian into rotating structures is due to the fact that a spatial symmetry breaking is associated with a supercritical Hopf bifurcation in the time domain. The rotation dynamics in these systems is realized through tunneling between lattice sites [15,16]. For parameters for which rotational dynamics occurs, we have analyzed solitonic solutions by using the modified Petviashvili’s method [17,18], and we have found the relation between rotating structures and solitonic solutions. Quite unexpectedly, it has been discovered that solitonic solutions, derived for the steady state of governing equations, can help in finding parameters of Gaussian-induced time-dependent rotation. All of this is done by considering square and hexagonal/trigonal PLs with a central defect (Fig. 1).

The behavior of CP beams in PLs is described by a time-dependent model consisting of wave equations in the paraxial approximation for the propagation of CP beams and a relaxation equation for the generation of the space charge field in the photorefractive

crystal. The model equations in the computational space (one  $x$  or  $y$  unit corresponds to  $8.5 \mu\text{m}$ , one  $z$  unit corresponds to  $4 \text{ mm}$ ) are [19]

$$i\partial_z F = -\Delta F + \Gamma EF, \quad -i\partial_z B = -\Delta B + \Gamma EB, \quad (1)$$

$$\tau\partial_t E + E = -\frac{I + I_g}{1 + I + I_g}, \quad (2)$$

where  $F$  and  $B$  are the envelopes of the forward and backward propagating beams.  $\Delta$  is the transverse Laplacian,  $\Gamma$  is the beam coupling constant, and  $E$  the homogenous part of the space charge field.  $I = |F|^2 + |B|^2$  is the laser light intensity, measured in units of the background intensity  $I_d$ .  $I_g$  is the intensity distribution of the optically induced lattice array.  $\tau$  is the relaxation time of the crystal, which also depends on the total intensity,  $\tau = \tau_0 / (1 + I + I_g)$ , and consequently on the spatial coordinates. The numerical procedure is as in Ref. [19].

We consider a lattice array with a square and trigonal arrangement of beams and with the central beam absent. We launch head-on CP Gaussian beams into the center of the lattice, parallel to the lattice beams. For both PLs we found very clear and periodical rotation (Fig. 2) in a very narrow region of the control parameters (see also movies at [20]). Each Gaussian beam collapses to a displaced solitonlike beam, and

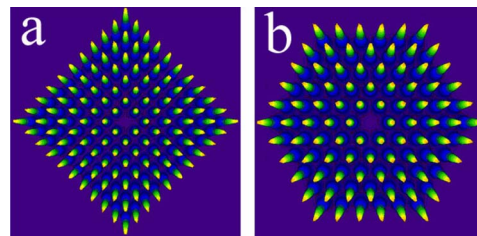


Fig. 1. (Color online) The considered periodic PLs. a, Square PL, given by  $I_g = I_0 \cos^2[\pi(x+y)/d] \cos^2[\pi(x-y)/d]$ ; lattice spacing  $d = 35 \mu\text{m}$ , maximum lattice intensity  $I_0 = 20I_d$ . b, Trigonal PL, formed by positioning Gaussian beams at the sites of the lattice; lattice spacing  $d = 28 \mu\text{m}$ , FWHM of lattice beams  $12.7 \mu\text{m}$ , maximum lattice intensity  $I_0 = 20I_d$ .

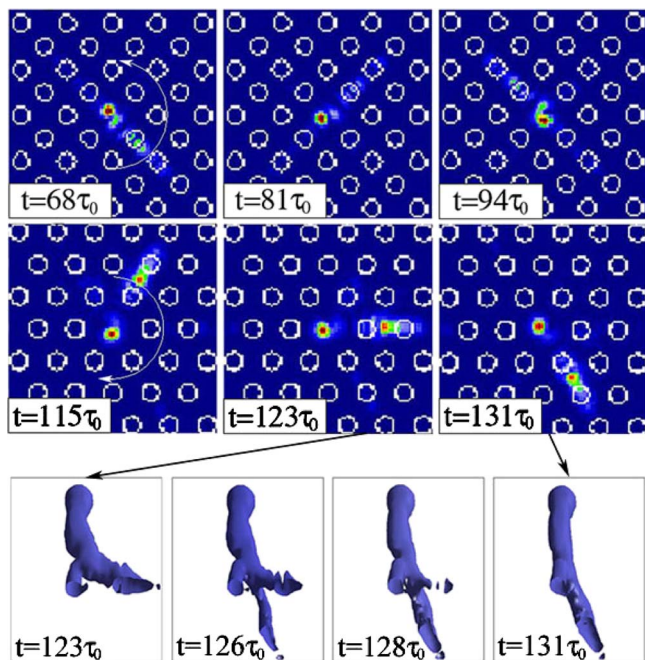


Fig. 2. (Color online) Gaussian-induced rotation: intensity distribution of backward beam at its exit face of the crystal, presented at different times. For the square PL (first row):  $\Gamma=27.6$ , input FWHM of CP Gaussian beams  $8.2 \mu\text{m}$ , beam power 2.08. For the trigonal PL (second row):  $\Gamma=25$ , input FWHM of CP Gaussian beams  $11 \mu\text{m}$ , beam power 3.80. In both cases the propagation distance is  $L=2L_D=8 \text{ mm}$  and  $|F_0|^2=|B_L|^2=1I_d$ . The third row shows isosurface plots of a rotating structure for the trigonal PL at characteristic times.

after transient dynamics they start to rotate indefinitely. Since for parameters of such stable periodic solutions there are no stable steady states and since, in numerics, Eq. (2) becomes equivalent to the scalar nonlinear delay differential equation, this phenomenon is recognized as supercritical Hopf bifurcation [21]. The central parts of Gaussians rotate regularly in the center of the lattice, owing to the defect, along the whole crystal. Filaments rotate with the constant period away from the center along symmetry axes of the lattice by tunneling between lattice sites, but only close to its exit face of the crystal. Gaussian-induced rotating structures present solitonlike solutions, because they preserve shape along the main symmetry direction during rotation. The physical origin beyond rotation is incoherent interaction and spontaneous symmetry breaking, while rotation is realized through Zener tunneling [15,16]. Zener tunneling is the natural effect in CP geometry, because each of the beams induces the transverse index gradient (ramp [16]) for the other. Observed rotating structures are stable in the presence of up to 5% noise added to the input beam intensity and phase. Spontaneous symmetry breaking via noise chooses the direction of rotation, both directions occur with 50% probability. For the same control parameters, CP Gaussian beams show very irregular dynamical behavior in the absence of any lattice, but very stable propagation is found in the lattices without defects (not shown).

For geometries and parameters that allow stable rotation, we investigate the existence of the solitonic 2D solutions. In order to do that, we consider Eqs. (1) and (2) in the steady state. Because of their symmetry, the above equations suggest the existence of a fundamental 2D vector soliton solution in the form

$$F = u(x,y)\cos(\theta)e^{i\mu z}, \quad B = u(x,y)\sin(\theta)e^{-i\mu z}, \quad (3)$$

where  $\mu$  is the propagation constant and  $\theta$  is an arbitrary projection angle ( $\theta=\pi/4$  here; the same analysis also corresponds to the copropagating geometry but with the choice  $\theta=0$ ). When this solution is substituted into Eqs. (1), they both transform into one, degenerate equation:

$$\mu u + \Delta u + \Gamma u \frac{|u|^2 + I_g}{1 + |u|^2 + I_g} = 0. \quad (4)$$

The solitonic solutions can be found from Eq. (4) by using the modified Petviashvili's iteration method. Here we just determine different classes of spatial vector solitons, assuming that they are stable and observable over certain crystal lengths.

Figures 3 and 4 show power diagrams together with the characteristic solitonic solutions for the cases of square and trigonal PLs, respectively. In the search for solitonic solutions, we used the same Gaussian input beams and parameters  $\Gamma$  as in the numerical simulations. We varied the propagation constant  $\mu$  to find the beam power ( $P = \int_{-\infty}^{\infty} \int_{-\infty}^{\infty} |u|^2 dx dy$ ) corresponding to the beam power of the stable rotating structures. We found powers for  $\mu=22.641$  ( $P=2.08$ ) and  $\mu=20.751$  ( $P=3.80$ ) for square and trigonal PLs, respectively (shown by appropriate profiles in Figs. 3 and 4). Such solitonic solutions could be found only in the very narrow region

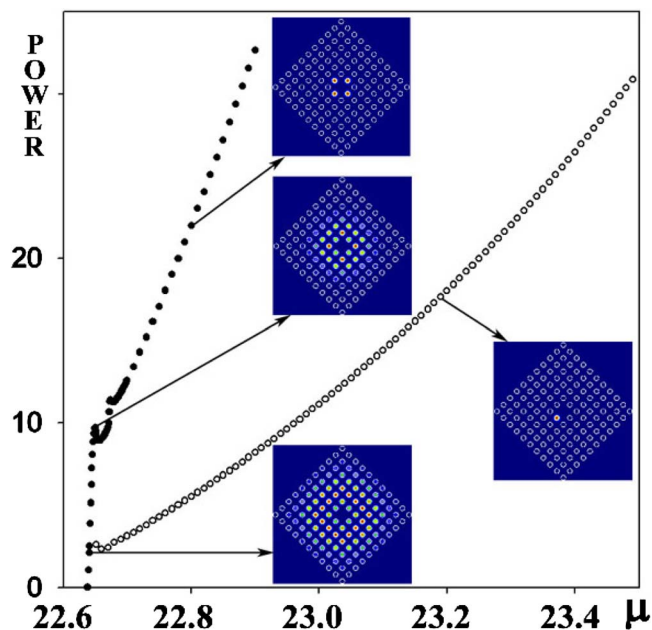


Fig. 3. (Color online) Power diagram of solitonic solutions for the square PL. Various symbols indicate different kinds of solitonic solution, characterized by corresponding profiles. Lattice parameters are as in Fig. 1, and  $\Gamma=27.6$ .

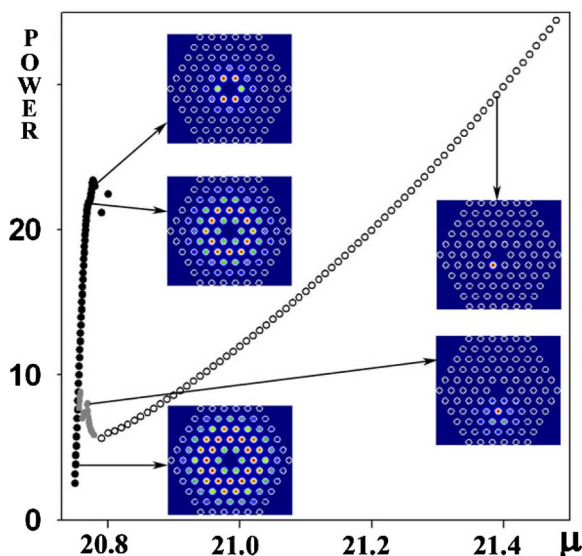


Fig. 4. (Color online) Power diagram of solitonic solutions for the trigonal PL. Various symbols indicate different kinds of solitonic solution, characterized by corresponding profiles. Lattice parameters are as in Fig. 1, and  $\Gamma=25$ .

near the lowest value of  $\mu$ . Of course, because of the CP geometry, these solitonic solutions are stable, but only up to some critical values of propagation distance [22]. In Figs. 3 and 4 we present only those intervals of  $\mu$ , since there are no solitons for lower values of  $\mu$ , while for larger values solitonic solutions are nonphysical owing to the very large peak intensity (in comparison with the maximum lattice intensity  $I_0$ ).

In power diagrams (Figs. 3 and 4) filled circles represent all characteristic types of symmetric discrete solitonic solution. By increasing the propagation constant  $\mu$  these solutions become more localized. Only for the beam powers corresponding to the less localized solitonic solutions can one find Gaussian-induced rotation in numerical simulations. Similar power diagrams are found for the same lattice geometries, but for different values of the coupling constant  $\Gamma$ . Again, the same types of symmetric discrete solitonic solution are found, and, for the beam powers corresponding to the less confined solitonic solutions, Gaussian-induced rotation can be found for some values of propagation distance. This procedure provides a more convenient way of finding Gaussian-induced rotation in numerics, as well as in experimental consideration of this interesting phenomenon.

In conclusion, we stress that, in contrast to the results given in the literature, where 2D spatial rotation in ring periodic lattices were discussed, we observed 3D time-dependent rotation in periodic PLs. For the parameters of such rotation, we found solitonic solutions that correspond to the lowest values of the propagation constant in the power diagrams. To find rotating structures for the discussed lattice geometry, it is more convenient to find less confined

symmetric solitonic solutions by varying propagation constant  $\mu$  and then, for the same coupling constant  $\Gamma$  and beam power, to look for the propagating distance for which rotation occurs, either in numerical simulations or in experiments. Moreover, we believe that our procedure is applicable, besides to Kerr-type nonlinearities, to any system that can be described by a modified nonlinear Schrödinger equation with a periodic potential, such as Bose–Einstein condensates in optical lattices.

Work at the Institute of Physics is supported by the Ministry of Science, project OI 141031.

## References

1. J. D. Joannopoulos, R. D. Meade, and J. N. Winn, *Photonic Crystals: Molding the Flow of Light* (Princeton U. Press, 1995).
2. N. K. Efremidis, S. Sears, D. N. Christodoulides, J. W. Fleischer, and M. Segev, *Phys. Rev. E* **66**, 046602 (2002).
3. D. N. Christodoulides, F. Lederer, and Y. Silberberg, *Nature* **424**, 817 (2003).
4. J. Fleischer, T. Carmon, M. Segev, N. Efremidis, and D. Christodoulides, *Phys. Rev. Lett.* **90**, 023902 (2003).
5. Y. S. Kivshar and G. P. Agrawal, *Optical Solitons: from Fibers to Photonic Crystals* (Academic, 2003).
6. D. N. Christodoulides, and R. I. Joseph, *Opt. Lett.* **13**, 794 (1988).
7. H. Eisenberg, Y. Silberberg, R. Morandotti, A. Boyd, and J. Aitchison, *Phys. Rev. Lett.* **81**, 3383 (1998).
8. J. W. Fleischer, M. Segev, N. K. Efremidis, and D. N. Christodoulides, *Nature* **422**, 147 (2003).
9. D. N. Neshev, T. J. Alexander, E. A. Ostrovskaya, Y. S. Kivshar, H. Martin, I. Makasyuk, and Z. Chen, *Phys. Rev. Lett.* **92**, 123903 (2004).
10. J. W. Fleischer, G. Bartal, O. Cohen, O. Manela, M. Segev, J. Hudock, and D. N. Christodoulides, *Phys. Rev. Lett.* **92**, 123904 (2004).
11. Y. V. Kartashov, V. A. Vysloukh, and L. Torner, *Opt. Lett.* **30**, 637 (2005).
12. X. Wang, Z. Chen, and P. G. Kevrekidis, *Phys. Rev. Lett.* **96**, 083904 (2006).
13. B. B. Baizakov, B. A. Malomed, and M. Salerno, *Phys. Rev. E* **74**, 066615 (2006).
14. M. S. Petrović, *Opt. Express* **14**, 9415 (2006).
15. H. Trompeter, T. Pertsch, F. Lederer, D. Michaelis, U. Streppel, A. Bräuer, and U. Peschel, *Phys. Rev. Lett.* **96**, 023901 (2006).
16. H. Trompeter, W. Krolikowski, D. Neshev, A. Desyatnikov, A. Sukhorukov, Y. Kivshar, T. Pertsch, U. Peschel, and F. Lederer, *Phys. Rev. Lett.* **96**, 053903 (2006).
17. V. I. Petviashvili, *Plasma Phys.* **2**, 469 (1976).
18. J. Yang, I. Makasyuk, A. Bezryadina, and Z. Chen, *Stud. Appl. Math.* **113**, 389 (2004).
19. M. Belić, D. Jović, S. Prvanović, D. Arsenović, and M. Petrović, *Opt. Express* **14**, 794 (2006).
20. <http://mail.phy.bg.ac.yu/~jovic/GaussRotation/>.
21. L. Larger, J. P. Goedgebuer, and T. Erneux, *Phys. Rev. E* **69**, 036210 (2004).
22. K. Motzek, Ph. Jander, A. Desyatnikov, M. Belić, C. Denz, and F. Kaiser, *Phys. Rev. E* **68**, 066611 (2003).